# MONITORING OF INCOMING SILICON PV WAFERS WITH MODIFIED SURFACE PHOTOVOLTAGE (SPV) MINORITY CARRIER DIFFUSION LENGTH METHOD

M. Wilson[1], A. Savtchouk[1], F. Buchholz[2], S. Olibet[2], R. Kopecek[2], K. Peter[2], and J. Lagowski[1]

[1]Semilab SDI LLC Tampa, FL 33612, USA; e-mail: mwilson@semilabsdi.com
[2]International Solar Energy Research Center - ISC Konstanz, Rudolf-Diesel Str.15 , D-78467 Konstanz, Germany

ABSTRACT: The noncontact ac-surface photovoltage technique is modified to enable reliable measurement of the minority diffusion length in incoming silicon PV wafers. The modifications to overcome very low SPV signal in wafers with saw damage include three elements; 1- increased photon flux in a range that still maintains advantages of low injection level; 2- elevated frequency light modulation with increased averaging that enhances signal to noise ratio and 3- thermal preconditioning of surface to create depletion layer SPV. The technique is tested using comparative measurements on Cz wafers and MC wafers with saw damage and after a saw damage removal etch. Consistently similar results were obtained before and after etching for diffusion length L, and for iron and boron-oxygen defect concentrations. The results demonstrate excellent repeatability that for a L of about 100µm is 0.1%. The repeatability data for Fe and boron-oxygen enable to evaluate defect detection limits in low e9 atoms/cm$^3$ range. To our knowledge, no other techniques can match such sensitivity for as-cut saw damaged wafers.
Keywords: SPV, Minority Carrier Diffusion Length, Incoming Wafers

## 1 OUTLINE OF THE APPROACH

Surface photovoltage based measurement of minority carrier diffusion length is widely used in silicon IC manufacturing for monitoring heavy metal contamination and micro-defects for evaluation of the cleanliness of crystal growth, IC processing tools and key integrated circuit processing steps.

An extension of the technique to silicon PV wafers has been successful in measuring wafers after etching; after diffusion; after passivation, and also for measurements on final solar cells.

In this paper, we present a version of SPV that has been developed in order to achieve a similar wafer level monitoring of minority carrier diffusion length for incoming silicon PV wafers. Emphasis is given to reliable measurements of the diffusion length, iron and boron-oxygen defects in as-cut wafers without saw damage removal and without any surface passivation.

There are two recognized advantages of SPV for as-cut wafers that can make it especially attractive among carrier lifetime techniques: 1- SPV uses different light penetrations and signal ratio that eliminates the effect of front surface recombination velocity; it also uses algorithm for calculation of L that corrects the effect of back surface recombination velocity, in the case of long diffusion length comparable to or larger than the wafer thickness; 2- SPV measurements are not a subject of ambiguity caused by injection level dependences and nonlinear effects that in other carrier lifetime techniques generate fundamental questions on the true meaning of the measured parameters.

The modified SPV technique is based on the most advanced version of the technique, referred to as Ultimate SPV. It uses digitally controlled illumination and signal detection. Simultaneous measurements of SPV signals, generated by light beams of different wavelengths, and different but high modulation frequencies, help to overcome the signal to noise issue. In addition, the approach introduces the best known surface preconditioning achieved with 200°C annealing, that is compatible with defect monitoring used to isolate boron-oxygen defects and Fe. The approach is confirmed in a series of measurements performed on the same wafers before and after saw damage removal etch.

## 2 RESULTS

Very good measurement stability and repeatability are demonstrated with this approach; for example, a 1$\sigma$ standard deviation of 0.10µm is obtained in 10 repeats for a Cz as-cut wafer with an average diffusion length of 96µm. To our knowledge such repeatability of 0.1% could not be achieved for saw damaged wafers in any other lifetime techniques. High repeatability leads in turn to precise determination of iron concentration and concentration of LID (Light-Induced Defects) from diffusion length differences after defect activation and deactivation.

The measurements were performed with a modified apparatus and a special SPV procedure using a Semilab PV-2000 tool equipped with automated optical Fe activation and accelerated LID station with robotic wafer handling.

The results presented include SPV diffusion length, bulk lifetime, Fe and LID concentrations for photovoltaic silicon Cz wafers and multicrystalline wafers measured as-cut with saw damage and then after typical alkaline etching for Cz wafers and acid etching for MC wafers. Very good agreement is shown for measurements before and after etching. For example, for diffusion lengths from 50µm to 170µm, the values before and after etching differ by less than 5% for wafer average and by only about 10% for individual sites. For Fe measurements in the typical range from mid 1E10cm$^{-3}$ to 1E12 cm$^{-3}$ the relative differences were about twice larger than that for diffusion length. This is consistent with the differential character of Fe measurements. LID results were similar to those for Fe.

## 3 CONCLUSIONS

Present results prove that the modified SPV diffusion length method provides a reliable means for contamination measurement on incoming as-cut silicon PV wafers. A previous study has already shown very effective application of the SPV method to measurements on wafers after diffusion, passivation, and on the final solar cells [1]. This, combined with the new capability of measuring as-cut and etched wafers, opens a means for

reliable tracing of iron contamination and LID level throughout the entire PV manufacturing process. To our knowledge, this practically important capability has not been demonstrated by any other lifetime based techniques. Regarding further development of the SPV method for in-line measurement, this may be possible for diffusion length only. The activation cycle for Fe and ALID requires minutes and is therefore compatible with off-line sampling approaches.

## 4 ADDITIONAL EXPLANATION

### 4.1 About the approach

The "Ultimate SPV" arrangement adopted in this work is shown in Fig. 1. High precision and speed in Ultimate SPV is achieved by simultaneous measurement of two SPV signals. Two beams with slightly shifted frequency of light intensity modulation, $\omega_1$ and $\omega_2$, generate ac-photovoltage signals, $V_1$ and $V_2$. These signals are monitored simultaneously using two inputs of a lock-in amplifier tuned to frequencies $\omega_1$ and $\omega_2$, respectively. Two light beams are of different wavelengths, $\lambda_1$ and $\lambda_2$, and they penetrate silicon to different depths $z_1$ and $z_2$, respectively. The SPV signal detected with a transparent capacitive electrode above the top surface tends to be larger for shorter light penetration depth. This effect is reduced by diffusion of excess carriers. Therefore, the signal ratio $V_1/V_2$ is used to determine the minority carrier diffusion length, L.

As pointed out above, the signal ratio, $V_1/V_2$, cancels the effect of wafer front surface recombination, giving SPV a advantage over other lifetime measurements that are sensitive to surface recombination. The patented "enhanced SPV" procedure enables to extract diffusion length values exceeding the wafer thickness. This has proven to be of importance for very thin PV wafers with long L, such as PV wafers after gettering, including final solar cells with low back-contact surface recombination.

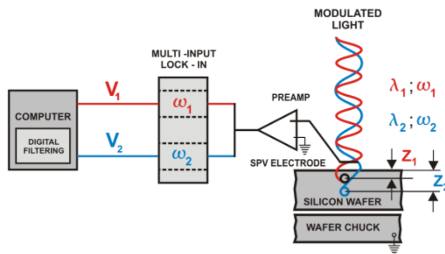


**Figure 1**. Illustration of "Ultimate SPV" arrangement for simultaneous measurement of two signals corresponding to different penetration depths z. L is determined from signal ratio $V_1(z_1)$ / $V_2(z_2)$, cancelling the effect of surface recombination, $S_{front}$. Algorithm with $S_{back}$ correction is used for long L.

In measuring as-cut PV wafers, the technique takes advantage of the unique frequency independent SPV signal that gives a steady-state condition in the high frequency range allowing the use of signal averaging. Simultaneous measurements of SPV signals generated by light beams of different wavelengths and different but high modulation frequencies help to overcome the signal to noise issue [2]. This is critical because as-cut wafers exhibit very low SPV signal (~10000 times lower than in etched wafers). The second element in the approach is the SPV signal enhancement achieved with preannealing of p-type saw damaged wafers.

The key to SPV measurement on as-cut wafers is overcoming the problem of signal to noise ratio. This is caused by a very low signal (see Fig. 2), about 4 orders of magnitude below signals on etched wafers commonly used in SPV metrology. This is overcome by using: 1- much higher light intensity that still corresponds to a low injection level and 2- use of high modulation frequency that in as-cut wafers is possible without entering into the frequency dependent range. The latter enables a large number of signal averaging without increasing of measurement time, and 3- use of thermal pretreatment that in p-type wafers increases the SPV signal.

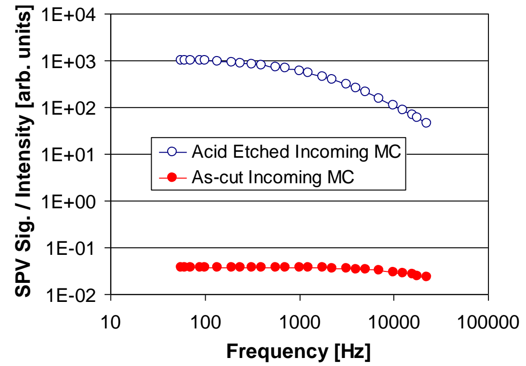


**Figure 2.** SPV signal vs. light modulation frequency that demonstrates much lower magnitude signal in the as-cut wafer that is practically independent of frequency.

Higher light intensity, increased frequency and simultaneous monitoring of two different wavelength SPV signals improve measurement stability and repeatability. This is demonstrated in Fig. 3 by a 0.1% standard deviation obtained in 10 repeats on an as-cut Cz silicon wafer 200µm thick. The 96µm diffusion length corresponds to low injection level bulk lifetime of about 4µs.

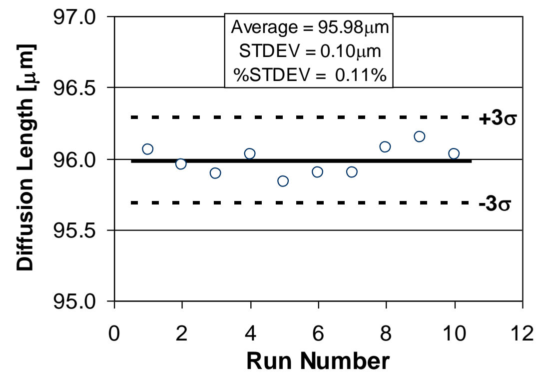


**Figure 3.** Repeatability of modified SPV diffusion length measurement on as-cut 200µm thick p-type Cz incoming wafer.

### 4.2 Preannealing and SPV mechanism in saw damaged wafers.

ac-SPV signal is detected between the capacitive electrode placed a fraction of a multimeter above the wafer and the back-side capacitive contact to the wafer provided by the wafer supporting chuck. Four possible contributions to surface photovoltage, $\Delta V_{SPV}$ are given in the equation below.

$$\Delta V_{SPV} = \Delta V_{Surf}^{Depl} + \Delta V_{Junction}^{Depl} + \Delta V_{SPV}^{Dember} + \Delta V_{SPV}^{Tauc} \quad (1)$$

Depletion layer modulation represents the best case scenario. The Dember voltage, caused by differences in electron and hole diffusivities, and the Tauc voltage, caused by resistivity gradients can have significant lateral components that can interfere with the SPV diffusion length measurement [3]. In silicon wafers, a desired surface depletion is created using appropriate etch, that is different for p-type and n-type silicon. A larger depletion layer photovoltage is also observed in etched PV silicon wafers. For p-type wafers, the surface depletion is due to net positive electric charge present at the surface. We have found that such possible charge is induced in saw damaged surface layers by brief 200°C preannealing. This result is illustrated in Fig. 4. Annealing induced positive charge is manifested as an increase in SPV signal in p-wafers and a decrease in n-wafers. Additional measurement of Kelvin-probe surface voltage confirmed positive surface charging.

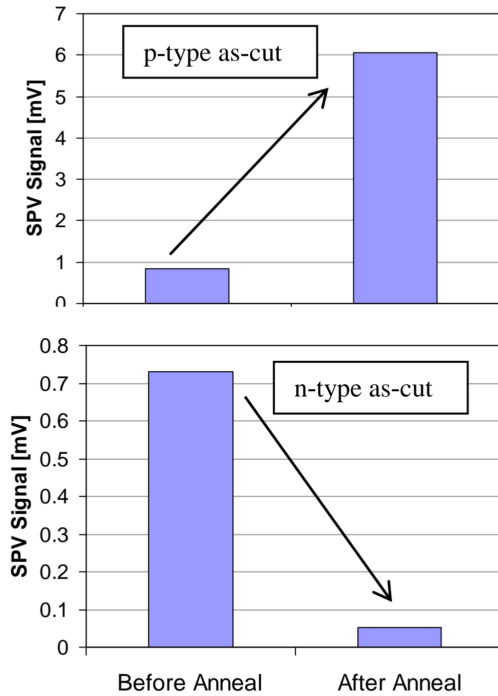


**Figure 4.** The effect of 200°C preannealing on SPV signal for as-cut silicon PV wafers with saw damage.

Based on our results, we can suggest 200°C preannealing as The Best Known Method, BKM for SPV signal conditioning for p-type as-cut wafers with saw damage. (Such annealing shall not be used for n-type wafers as it decreases the SPV signal).

One shall notice that 200°C preannealing is used as a LID annihilation treatment. Therefore, it incorporates well into boron-oxygen and Fe monitoring sequence.

4.3 Applications of the Approach to Incoming Wafers

For defect determination (Fe, boron-oxygen related LID defects), the ac-SPV measurements are performed at certain stages of selective defect activation-deactivation that involve optical and thermal wafer treatments performed in an automatic sequence using the Accelerated Light Induced Degradation Station, ALID described in ref 1. Defect concentration is determined from a change of $1/L^2$ with a precalibrated coefficient for Fe.

For Fe in atoms/cm$^3$, the specific equation is

$$[Fe] = 1.05e16\,[L_{Aft}^{-2} - L_{Bef}^{-2}] \quad (2)$$

where $L_{Aft}$ and $L_{Bef}$ are the diffusion lengths in µm after selective activation of Fe recombination and before activation, respectively. Concentration of other defects is given as an "iron equivalent" concentration. The iron equivalent boron-oxygen LID concentration in defects/cm$^3$ is calculated as

$$[LID] = 1.05e16\,[L_{Act}^{-2} - L_{DeAct}^{-2}] \quad (3)$$

where $L_{Act}$ and $L_{DeAct}$ are the diffusion lengths in µm after selective activation and deactivation of boron-oxygen centers.

The minority carrier diffusion length value is a bulk quality sensitive parameter. In sampling measurements, illustrated in Fig. 5, it confirms the expected quality degradation in the top position of multicrystalline ingot and to a lesser degree at the bottom of the ingot.

On the bottom of Fig. 5 this tendency is also seen in iron concentration that was measured using L values before and after optical Fe activation. Results in Fig. 5 also demonstrate very similar values of L and Fe obtained before and after a saw damage removal acid etch. Note that all Fe and LID measurements were done for p-type B-doped wafers.

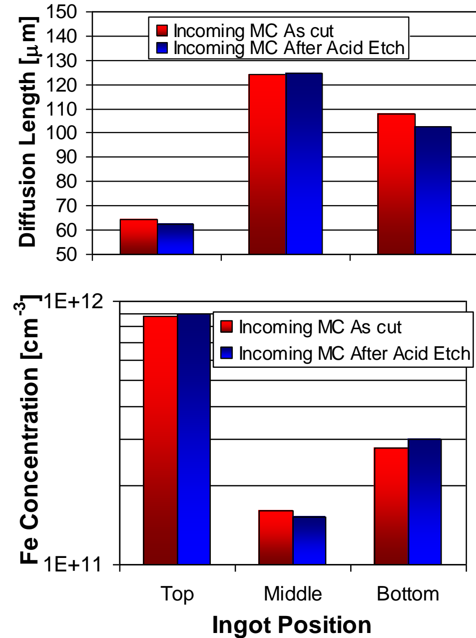


**Figure 5.** Wafer average values in SPV sampling measurements for 3 multicrystalline ingot positions. Results before and after etching are for the same wafers.

Application of the approach to p-type Cz incoming wafers are illustrated in Fig. 6 by the results of L, Fe and LID data measured on 9 wafer sites before and after etching. The use of the ALID station in the PV-2000 tool enables separation between Fe and boron-oxygen LID defects [1].

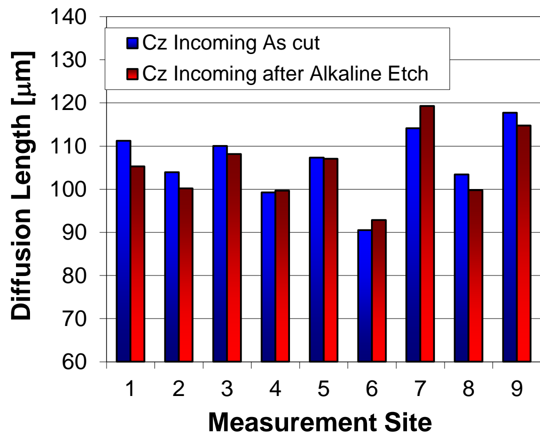


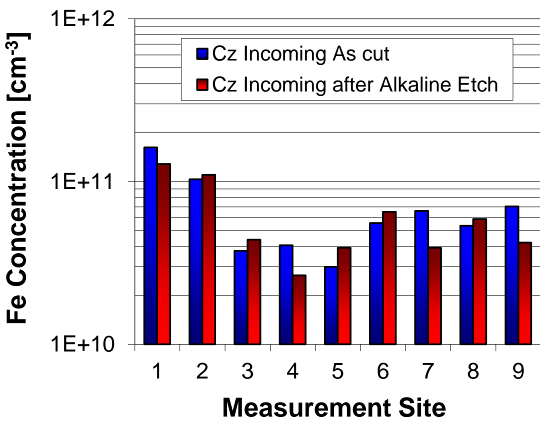


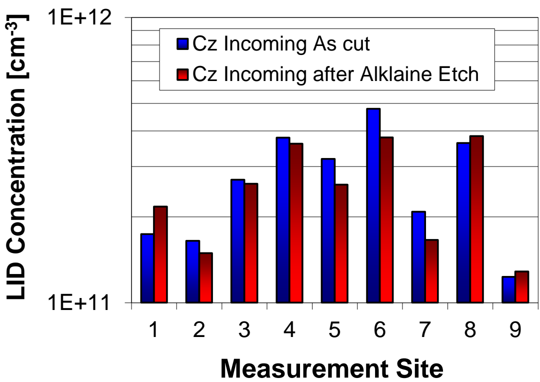


**Figure 6.** Results measured on 9 sites of a p-type Cz wafer, as-cut and after etching.

A comparison of Fe and LID before and after etching for both MC and Cz p-type incoming wafers was performed for many samples from multiple vendors. Fig. 7 presents a correlation of Fe and LID before and after etching for 5 such wafers (9 sites each). Good correlation is observed even down into the low 1e10 $cm^{-3}$ range for both Fe and LID indicating a resolution of the technique for as-cut wafers down into 1e9 $cm^{-3}$ range.

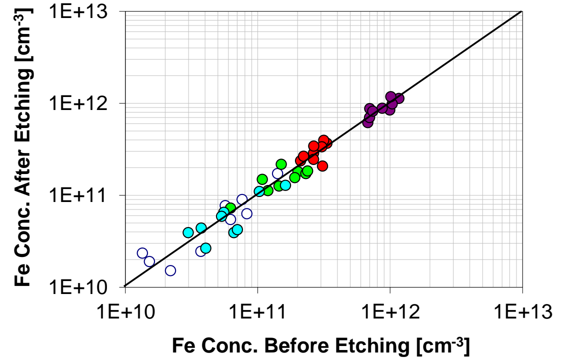


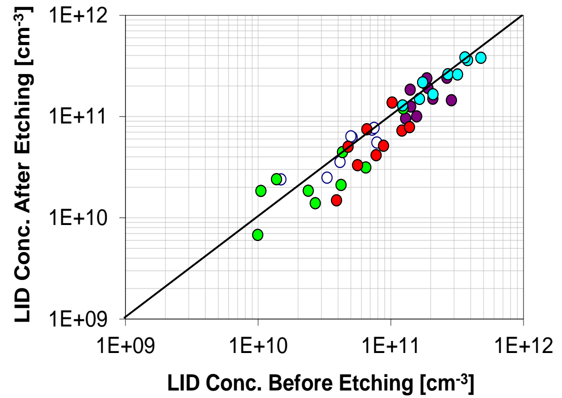


**Figure 7.** Correlation of Fe and LID before and after saw damage removal etch for both MC and Cz p-type incoming wafers.

4.3 Wafer Mapping

The SPV technique enables to perform whole wafer mapping of the diffusion length, Fe and LID concentrations. The Fe and LID results obtained for a p-type, as-cut MC wafer are shown in Fig. 8.

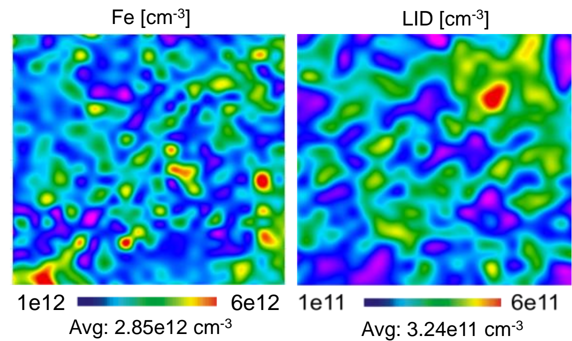


**Figure 8.** The map of SPV Fe and LID measured on a as-cut MC-wafer.

The averaging required in the case of very low SPV signal increases mapping time and becomes a limiting factor for Fe mapping in as-cut wafers. PV wafers with boron concentrations in 1E16 $cm^{-3}$ range should be measured in time below 5 min to prevent error caused by iron-boron pairing after activation. At present this limits the SPV Fe mapping in as-cut wafers to a low density matrix, 9x9 sites.

## 5. Comments on the Results

Similarity of SPV results on as-cut and etched wafers observed for all 3 quantities, i.e., diffusion length, iron concentration and LID concentration is an important finding; however, it is empirical in nature. Very similar values of SPV signal ratios were measured before and after etching in spite of large differences in absolute signal value. The similar before and after etching ratios were measured for all stages of diffusion length altering by defect activation / deactivation. These results seem to imply some kind of similarity between the effect of surface texturing and the effect of saw damage. Perhaps further study shall help to explain these findings.

## 6. References

[1] M. Wilson et al. **J. Electron. Mater., 39 (6)** 642-647 (2010).

[2] M. Wilson et al. **ECS Transactions, 16 (6)** 285-301 (2008).

[3] S. Sikorski, **Progress in Quantum Electronics, 27 (5)** 295-365 (2003).